Sensors and Actuators B 194 (2014) 503–510

Contents lists available at ScienceDirect

Sensors and Actuators B: Chemical

journal homepage: www.elsevier.com/locate/snb

Effects of N_2 and O_2 annealing on the multianalyte biosensing characteristics of CeO_2-based electrolyte–insulator–semiconductor structures

Chyuan Haur Kao[a], Hsiang Chen[b,*], Ming Ling Lee[c], Che Chun Liu[a], Herng-Yih Ueng[a], Yu Cheng Chu[b], Ching Bang Chen[b], Kow Ming Chang[c]

[a] Department of Electronic Engineering, Chang Gung University, Taoyuan 333, Taiwan, ROC
[b] Department of Applied Materials and Optoelectronic Engineering, National Chi Nan University, Puli 545, Taiwan, ROC
[c] Department of Electronic Engineering, National Chiao Tung University, Hsin-Chu 300, Taiwan, ROC

ARTICLE INFO

Article history:
Received 30 October 2013
Received in revised form
25 December 2013
Accepted 26 December 2013
Available online 4 January 2014

Keywords:
CeO_2
O_2 and N_2 annealing
Electrolyte–insulator–semiconductor
Material quality
Sensing performance

ABSTRACT

A CeO_2-based multi-analyte electrolyte–insulator–semiconductor (EIS) biosensor has been fabricated on silicon substrate. To enhance the material quality and sensing performance, annealing treatment in N_2 and O_2 ambient has been incorporated. To examine the annealing effects, material analyses were conducted using X-ray diffraction (XRD), X-ray photoelectron spectroscopy (XPS) and atomic force microscopy (AFM) to identify optimal treatment conditions. Furthermore, sensing performance for various ions of Na^+, K^+, urea, and glucose has also been tested. Results indicate that the membrane annealed at 800 °C in O_2 ambience exhibited a better performance with higher multianalyte sensitivity and a lower drift rate compared with the membrane annealed in N_2 ambience. Oxygen in O_2 ambience may cause stronger reflow and fill in the oxygen vacancy so that the material properties and sensing capability can be improved in O_2 annealing ambience.

1. Introduction

Ion sensitive field effect transistors (ISFETs) used for pH detection were first demonstrated by Bergveld in the 1970s [1]. The device substituted the fragile glass electrode with metal oxides when measuring pH values for various concentrations [2]. Modern ISFETs offer specific advantages in terms of small size, low impedance, solid-state structure and multiple ion sensing capability, making them popular devices for ion activity vivo surveys in biomedical processes. Developed from ISFETs, electrolyte insulator semiconductor (EIS) sensors have neither source nor drain. Because of their simple structure and manufacturing ease, they are considered a fundamental device for silicon-based field-effect chemical and biological sensors [3]. To fabricate an EIS device, various kinds of high-*k* metal oxide materials including Al_2O_3, Ta_2O_5, and WO_3 have been used [4–7]. Unfortunately, their structures are not generally stable enough for long-term, high-temperature applications because of the interfacial layer between the high-*k* metal oxide and the silicon used in their manufacture. The interface layer is not only the most critical part of an EIS sensor that can affect performance, it is also vital to overall sensor properties, as a flaw in the interface layer can often render the sensor inoperable. It is therefore necessary to explore new materials and alternative processes to mitigate interfacial defects. Rare-earth (RE) metals provide an alternative to traditional metal oxides providing a thinner interfacial layer, higher capacitance value and lower leakage current [8,9]. Among the rare-earth oxides, CeO_2 allows a wide band gap of 3.19 eV, has great mechanical strength, good redox properties [10], and has been used for gas and humility sensors [11,12].

Fabrication of CeO_2-based biosensors has been proposed by Ansari et al., who prepared glucose sensors using sol–gel methods [13], and Faisal et al., who proposed ethanol sensors consisting of CeO_2 [14]. However, a CeO_2 EIS sensing membrane has not yet been reported. In 2002, Nishikawa et al. demonstrated the high performance CeO_2 dielectrics, pointing to their good interfacial properties on Si substrate [15]. In this study, CeO_2 has been sputtered on Si substrate as the sensing membrane for EIS sensing applications. In addition to traditional pH sensing capability, the sensing performance of the CeO_2 EIS structure in various solutions containing Na^+, K^+, urea, and glucose [16–18] were examined for future industrial multi-analyte biosensor applications. Moreover, the effects of post rapid thermal annealing (RTA) treatment in

* Corresponding author. Tel.: +886 49 2424905; fax: +886 49 2912238.
E-mail address: hchen@ncnu.edu.tw (H. Chen).

0925-4005/$ – see front matter © 2014 Elsevier B.V. All rights reserved.
http://dx.doi.org/10.1016/j.snb.2013.12.103

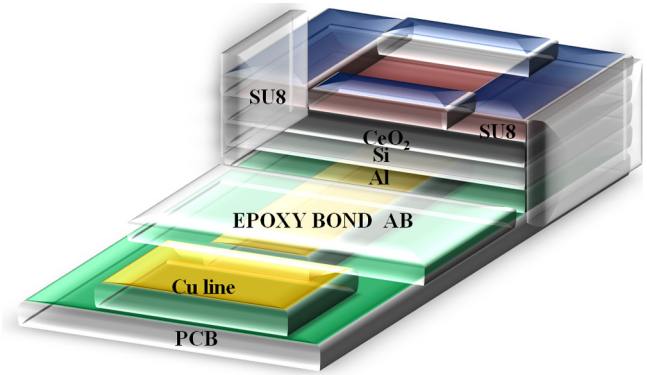

Fig. 1. CeO_2—based EIS structure.

distinct ambience of N_2 and O_2 [19,20] on the material properties and the sensing performance were examined because appropriate annealing could improve the material quality and optimize the sensing performance [21]. According to previous reports, O_2 annealing could cause stronger atoms reflow during annealing [22]. Furthermore, oxygen vacaices could be filled-in by the oxygen in O_2 ambient [23]. Therefore, multianalyte sensing capability of the membrane with O_2 annealing performed better than the membrane with N_2 annealing treatment.

2. Experiment

To incorporate CeO_2 membranes on EIS structures, fabrication was performed on a 4-inch n-type (1 0 0) Si wafer with a resistivity of 5–10 Ω cm. To remove the native oxide, the wafers were cleaned using HF-dip (HF:H_2O = 1:100) before deposition on the CeO_2 film. Then, 50 nm CeO_2 was deposited on the silicon wafer by radio frequency (RF) reactive sputtering with a mixture of Ar and O_2 (Ar:O_2 = 25:0) ambient during sputtering. The RF power was 150 W and the ambient pressure was 20 mTorr. RTA was used to anneal the samples at different temperatures of 600, 700, 800 and 900 °C in O_2 ambient for 30 s. Other samples were annealed at the same RTA temperatures and conditions in N_2 ambient. An Al film of 300 nm in thickness was then deposited on the backside of the Si wafer. Next, a photosensitive epoxy (SU8-2005 of MicroChem Inc) was used to define the sensing area through a standard photolithography process. Finally, the samples were fabricated on the copper lines of printed circuit board (PCB) in silver gel. A detailed EIS structure is illustrated in Fig. 1.

3. Result and discussion

3.1. Material analysis

Fig. 2(a) and (b) show the XRD patterns of the cerium oxide layer treated with RTA in N_2 and O_2 ambient, respectively. The crystalline phase of CeO_2 of the as-deposited sample can clearly be observed to have the characteristic peaks of XRD and three diffraction peaks of (2 0 0), (2 2 0) and (3 1 1), which can be observed at 33.07°, 47.83° and 56.78° for both treatments. In Fig. 2(a) of the samples treated in N_2 ambient, when the temperature rose to 800 °C, the peaks at (2 0 0) and (2 2 0) increased in intensity. This phenomenon might be caused by the enhancement of lattice structures in different temperatures forming higher peak intensities. Moreover, the peak intensity increased as the temperature rose, becoming strongest when reaching an RTA temperature of 800 °C, clearly exhibiting a stronger peak at (2 0 0), and then suddenly decreasing at 900 °C. This could be attributed to likelihood of the bonds of cerium and oxygen being destroyed when the CeO_2 film annealed at 900 °C. To

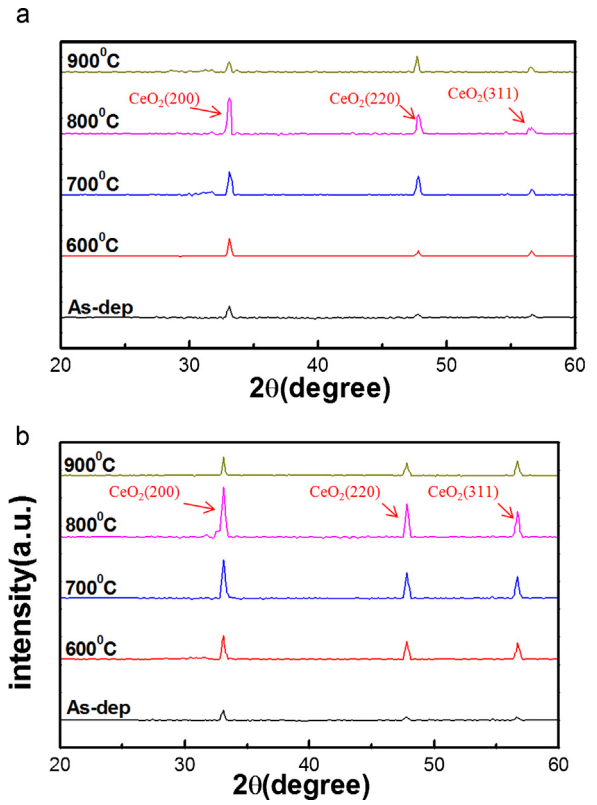

Fig. 2. XRD of the CeO_2 film after annealing at various temperatures on single crystalline silicon (a) in N_2 ambient (b) in O_2 ambient.

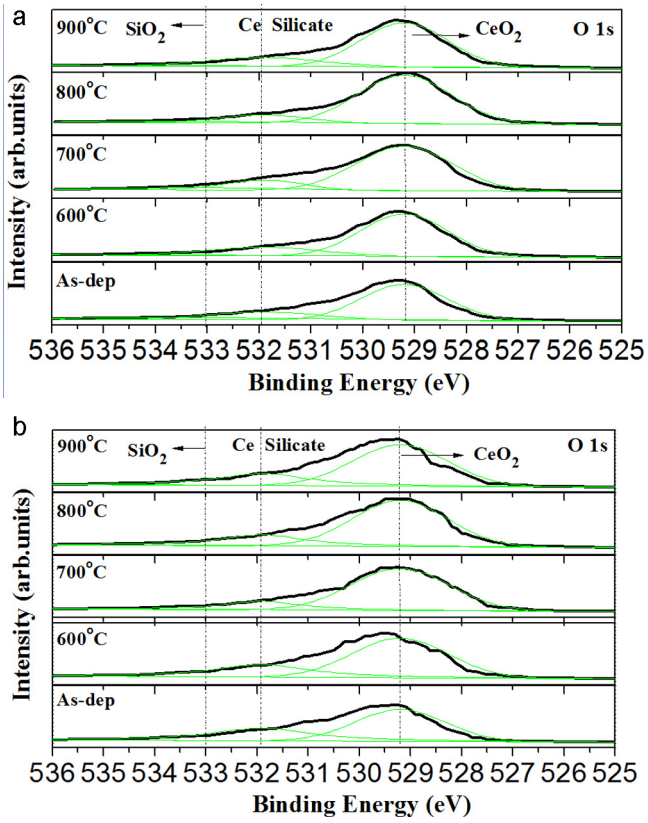

Fig. 3. The O 1s XPS results of CeO_2 film annealed (a) in N_2 ambient and (b) in O_2 ambient.

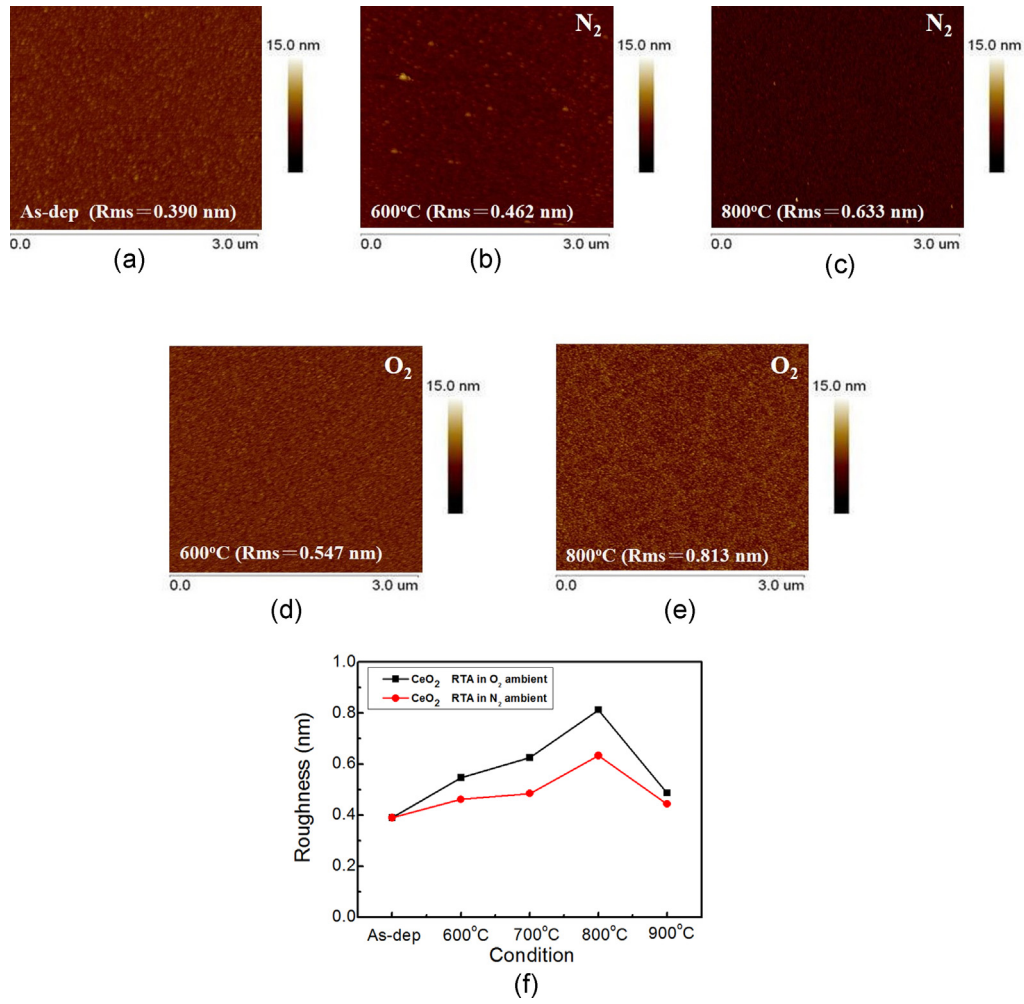

Fig. 4. AFM images of (a) the as-deposited film, (b) the film annealed at 600 °C in N_2 ambient (c) the film annealed at 800 °C in N_2 ambient (d) the film annealed at 600 °C in O_2 ambient and (e) the film annealed at 800 °C in O_2 ambient. (f) Comparison of AFM analysis for CeO_2 annealed at various temperatures in different gas (N_2 or O_2) ambient on single crystalline silicon.

compare RTA treatments in N_2 and O_2 ambient, In Fig. 2(b) of the samples treated in O_2 ambient, it can be observed that during peaks (2 0 0) and (2 2 0) intensities increased more in the O_2 ambient, while peak (3 1 1) intensity increased much more than the samples treated in N_2 ambient. The drastic increase of peak (3 1 1) might be due to the fact that O_2 annealing caused oxygen atoms filled in more oxygen vacancies than N_2 annealing, leading to higher peak intensity [23]. By comparing Fig. 2(a) and (b), it can be confirmed

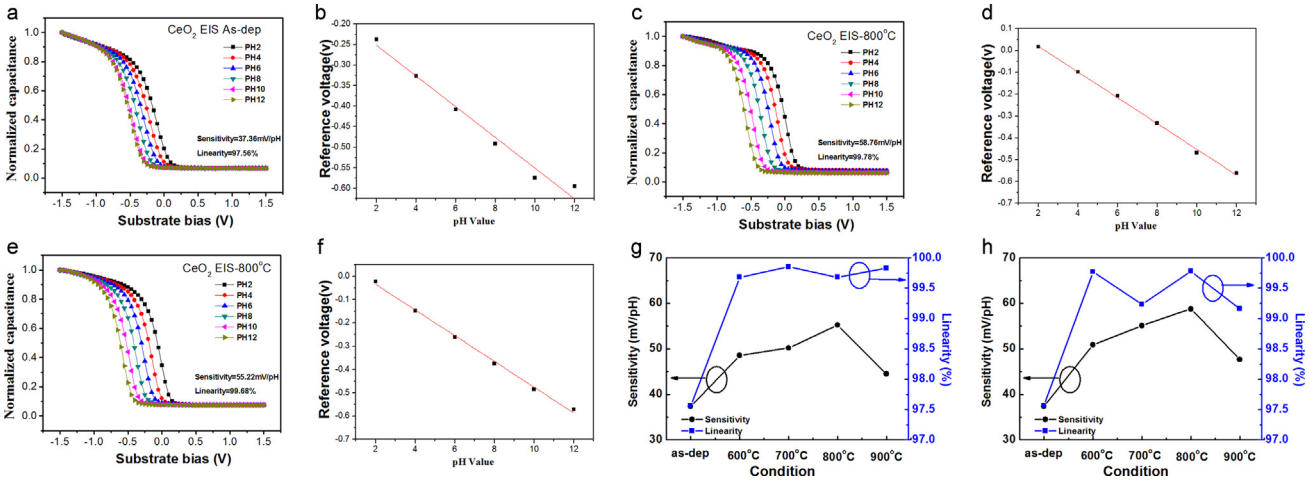

Fig. 5. (a) *C–V* curves for pH detection of the as-deposited CeO_2 sensing membrane and (b) the extracted sensing performance (c) *C–V* curves for pH detection of the CeO_2 sensing membrane annealed at 800 °C in N_2 ambient and (d) the extracted sensing performance (e) *C–V* curves for pH detection of the CeO_2 sensing membrane annealed at 800 °C in O_2 ambient and (f) the extracted sensing performance (g) sensitivity and linearity CeO_2 sensing membrane with various RTA temperatures in N_2 ambient (h) sensitivity and linearity CeO_2 sensing membrane with various RTA temperatures in O_2 ambient.

that the CeO_2 sensing membrane after post-RTA treatment in O_2 not only formed a stronger lattice structure, enhancing the peak intensity, but also better stabilized the crystalline structure than the post-RTA treatment in N_2 sample.

X-ray photoelectron spectroscopy (XPS) was employed to investigate the chemical-binding states in the CeO_2 sensing membrane on the Si substrate. Fig. 3(a) and (b) shows the O 1s spectra of the as-deposited samples and those formed by RTA annealing in N_2 and O_2 ambient, respectively. The O 1s spectra for the as-deposited and annealed films include the appropriate three-peak curve-fitting lines. In the spectra, the O 1s peak at 529.2 eV represents the CeO_2 bond, and the intermediate binding energy (531.9 eV) is attributed to Ce silicate represented by the Si–O–Ce bond. The highest binding energy (533 eV) is assigned to SiO_2 representing the Si–O bond. As the as-deposited samples show a strong Ce-silicate and low SiO_2 peak, and the samples which underwent post-RTA treatment in N_2 and O_2 at 800 °C show stronger bonding intensity for CeO_2 and a weaker O 1s peak for Ce–silicate than other samples. The results indicate that appropriate annealing at 800 °C both in N_2 and O_2 ambient could effectively suppress the formation of Ce silicate and SiO_2. However, as the annealing temperature increased to 900 °C, the concentration of Ce silicate and SiO_2 increased again both in N_2 and O_2 annealing because Si atoms might react with CeO_2 at a high annealing temperature of 900 °C [21].

To examine the surface morphologies for the CeO_2 films, atomic force microscopy (AFM) was used to monitor the surface. The surface morphologies of the sensing membranes were measured by Veeco D5000 AFM in tapping mode using an applied Nano silicon tip with a 50 N/m spring constant. The scan rate was 1 Hz, the scan area was 3 × 3 μm, and the set engagement ratio was 80%. To reveal the surface roughness, Fig. 4(a) shows the surface for the as-deposited film, Fig. 4(b) and (c) show the surface for the film annealed in N_2 ambient at 600 and 800 °C, and Fig. 4(d) and (e) show the surface for the film annealed in O_2 ambient at 600 and 800 °C. To illustrate the trend of the annealing conditions, Fig. 4(f) show the roughness of the CeO_2 films for the as-deposited and post-RTA films treated in N_2 and O_2 ambient, respectively. In both ambient, the CeO_2 film annealed at 800 °C had the highest surface roughness indicating, crystallization-induced large grains might be formed with annealing. Furthermore, the roughness of the CeO_2 film annealed in O_2 ambient was larger than the film annealed in N_2 ambient. The results imply that fewer dangling bonds and traps might exist in the film annealed in O_2 ambient than the film annealed in N_2 ambient because stronger reflow in O_2 ambient and repairing the oxygen vacancies by O_2 might improve material quality the CeO_2 film [22,23].

3.2. pH sensing capability

The flat band voltage shift of the *C–V* curve due to the change in the concentration of hydrogen ions was applied to detect the pH value of solutions. To evaluating the sensing performance, pH sensitivity of the EIS structures with CeO_2 sensing membranes without annealing, with annealing in N_2 ambient and O_2 ambient were measured, respectively. The *C–V* curves of the EIS structures with the as-deposited membrane, the membrane annealed at 800 °C in N_2 ambient and O_2 ambient are shown in Fig. 5(a), (c) and (e). Extracted from the CV curves, the reference capacitance shift of the CeO_2 membrane reveals that the sensitivity and linearity of the as-deposited membrane, the membrane annealed in N_2 ambient and O2 ambient were 37.36 mV/pH and 97.56%, 55.22 mV/pH and 99.68%, and 58.76 mV/pH and 99.78%, as shown in Fig. 5(b), (d) and (f), respectively. In addition, the linearity and sensitivity of the EIS structure treated at various temperatures in N_2 ambient and O_2 ambient are shown in Fig. 5(g) and (h). The results indicate that annealing at 800 °C could enhance the pH sensing capability.

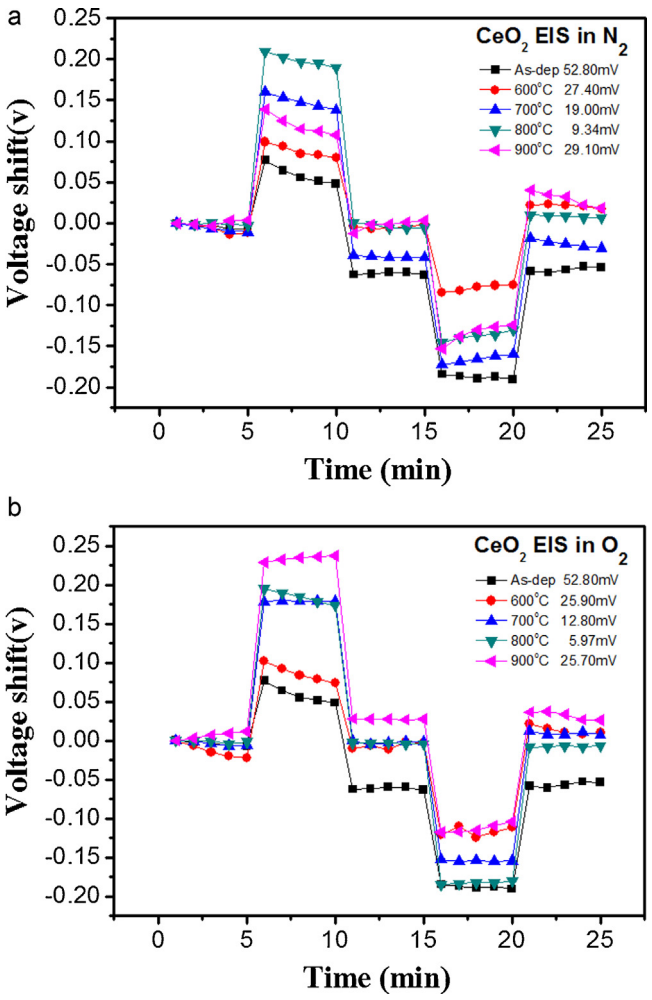

Fig. 6. (a) Hysteresis voltages for pH detection of CeO_2 sensing membrane with various RTA temperatures in N_2 ambient (b) Hysteresis voltages for pH detection of CeO_2 sensing membrane with various RTA temperatures in O_2 ambient.

Furthermore, O_2 annealing had the best sensing performance, which was consistent with all the material analyses. O_2 annealing at 800 °C could effectively reduce the vacancies and eliminate the dangling bonds. Therefore, the pH sensing capability could be optimized.

To examine the hysteresis effects of the membrane in various annealing conditions, the samples were immersed in buffer solutions of different pH values in an alternating cycle (pH7, pH4, pH7, and pH10) for 5 min for each solution. The above samples were subjected to a pH loop of 7 → 4 → 7 → 10 → 7 over a period of 25 min. Hysteresis voltage is defined as the gate voltage difference between the initial and the terminal voltages measured in the above pH loop. Fig. 6(a) and (b) shows the hysteresis effects of the samples treated at various annealing temperatures in N_2 ambient and O_2 ambient. In N_2 ambient and O_2 ambient, the sample annealed at 800 °C had the lowest hysteresis deviation. Furthermore, the sample annealed at 800 °C in O_2 ambient had the smallest hysteresis voltage of 5.97 mV. Since the defects and vacancies of the membrane might cause ions to attach on the surface, which might delay the reference voltage response [24]. An appropriate annealing at 800 °C with oxygen treatment might fill in the oxygen vacancies and dangling bonds to reduce attached ions on the surface during the test.

To investigate the drift rate of the membrane for long-time operations, the samples were immersed in pH7 buffer solutions for 12 h. The drift rate of the CeO_2-based EIS structure with membrane

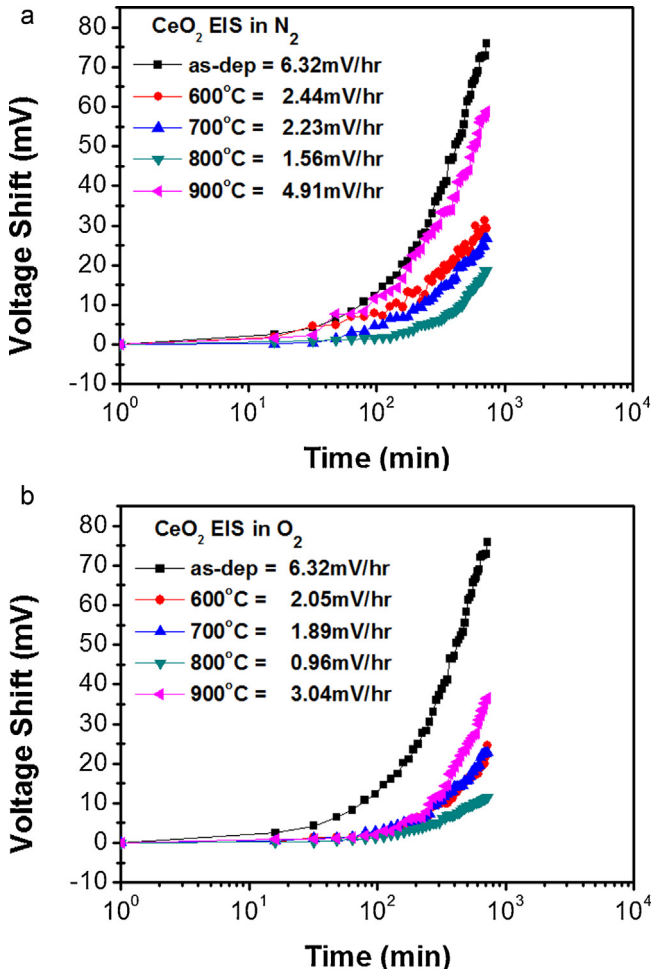

Fig. 7. Drift voltages for pH detection of CeO_2 sensing membrane annealed with various RTA temperatures (a) in N_2 ambient (b) in O_2 ambient.

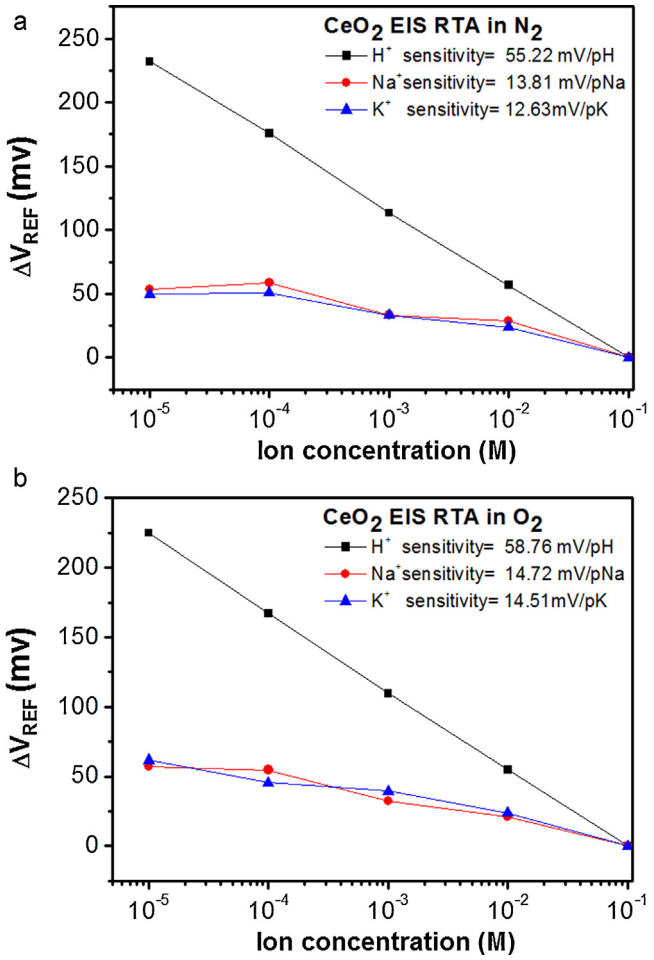

Fig. 8. H^+, Na^+, and K^+ ion sensitivity of (a) the membrane annealed at 800 °C in N_2 ambient (b) the membrane annealed at 800 °C in O_2 ambient.

annealed at various temperatures in N_2 ambient and O_2 ambient are shown in Fig. 7(a) and (b). The drift rate of the as-deposited sample and the sample annealed at 800 °C in N_2 ambient and O_2 ambient were 6.32, 1.56, and 0.96 mV/h, respectively. Among all the annealing conditions, the CeO_2 membrane annealed at 800 °C had the smallest drift rate. Since the defects such as vacancies and dangling bonds might capture clusters of ions and cause the reference voltage drift based on a model of gate voltage drift of pH-ISFET [25,26]. O_2 annealing could effectively remove those defects, which might worsen the sensing performance.

3.3. Multianalyte sensing performance

To investigate the properties of sensing film with different conditions in the potassium and sodium solution, 1 M NaCl/Tris–HCl and 1 M KCl/Tris–HCl were injected into buffer electrolyte by a micropipette. The concentrations of sodium and potassium ions were controlled in a range between 10^{-5} and 10^{-1} M. The pNa of CeO_2 samples with as-deposited and annealed samples at 800 °C in O_2 and N_2 ambient were 11.62, 14.72, and 13.81 mV/pNa, and the pK of CeO_2 samples with as-deposited and annealed samples at 800 °C in O_2 and N_2 ambient were 11.46, 14.51, and 12.63 mV/pK. Consistent with pH sensing results, O_2 annealed samples had higher sensitivity and linearity than N_2 annealed samples. In addition, the CeO_2 sensing films annealed at 800 °C in O_2 and N_2 ambient were more responsive to H^+ than to Na^+ and K^+, as shown in Fig. 8(a) and (b).

By incorporating suitable enzymes into the pH membranes, urea detection and glucose sensing biosensors can also be created [27–31]. Since enzymatic reactions usually produce ion species, ion-selective membranes with appropriate enzymes can measure variations in electrical signals caused by enzyme-catalyzed reactions, which can change ion concentration. After setting the process of enzyme immobilization by a covalent binding method, changes in pH hydrolysis of urea [32] or glucose [33] can be detected. The urea and glucose hydrolysis equations are written as Eqs. (1)–(3).

$$NH_2CONH_2 + 3H_2O \xrightarrow{\text{urease}} 2NH_4^+ + OH^- + HCO_3^- \quad (1)$$

$$\beta\text{-D-glucose} + O_2 + H_2O \xrightarrow{\text{glucose oxidase}} \text{D-glucose-}\delta\text{-lactone} + H_2O_2 \quad (2)$$

$$\text{D-glucose-}\delta\text{-lactone} \rightarrow \text{D-gluconoate} + H^+ \quad (3)$$

To analyze the urea sensing properties of the CeO_2 sensing membrane on the EIS structure, the urea solution with a concentration in a range between 5 and 40 mM was prepared. The urea sensing properties are shown in Fig. 9(a) and (b). The sensibility values of the as-deposited sample and annealed samples with RTA at 800 °C in O_2 and N_2 ambient were 2.35, 6.43, and 3.76 mV/mM, respectively. The linearity values of the as-deposited sample and annealed samples with RTA at 800 °C in O_2 and N_2 ambient were 84.38%, 93.83%, and 93.96%, respectively. It can be seen that the CeO_2 sensing membrane after RTA treatment at 800 °C in O_2 ambient had higher urea

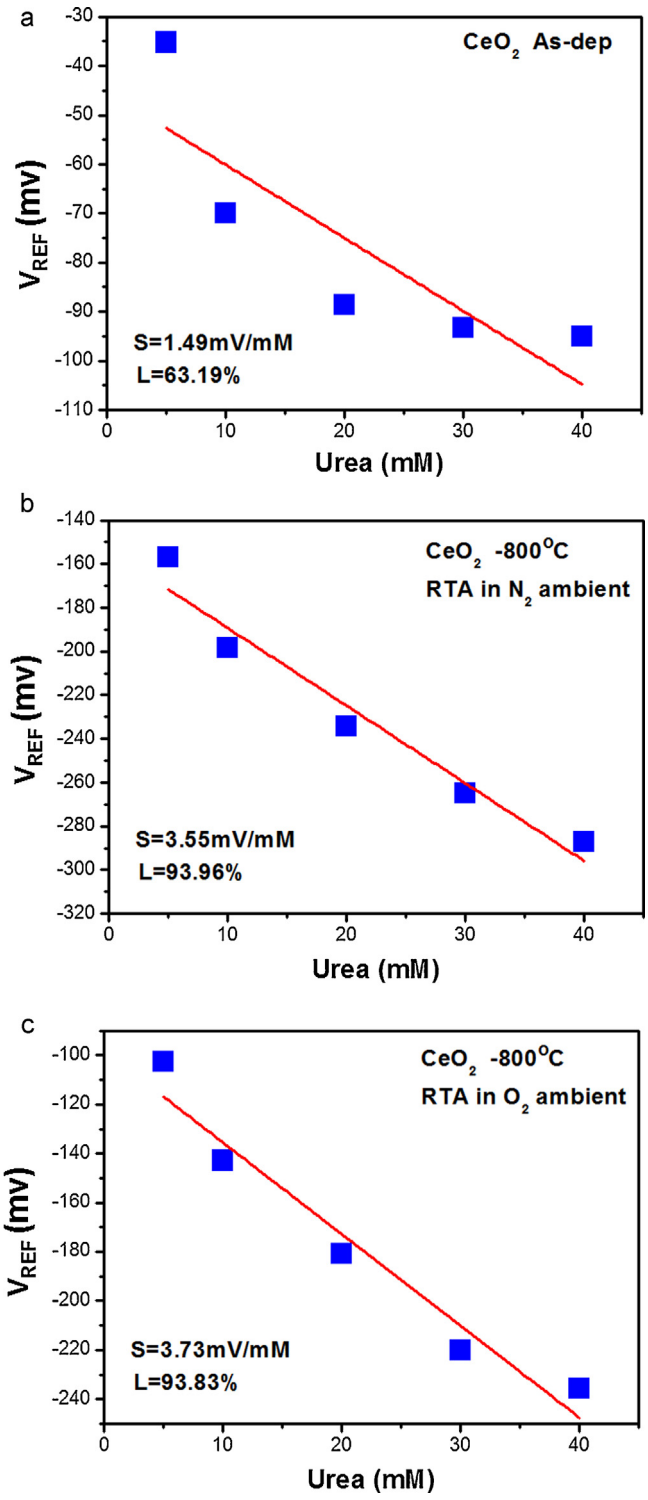

Fig. 9. Urea responses from (a) the as-deposited CeO_2 sensing membrane (b) the membrane annealed at 800 °C in N_2 ambient (c) the membrane annealed at 800 °C in O_2 ambient.

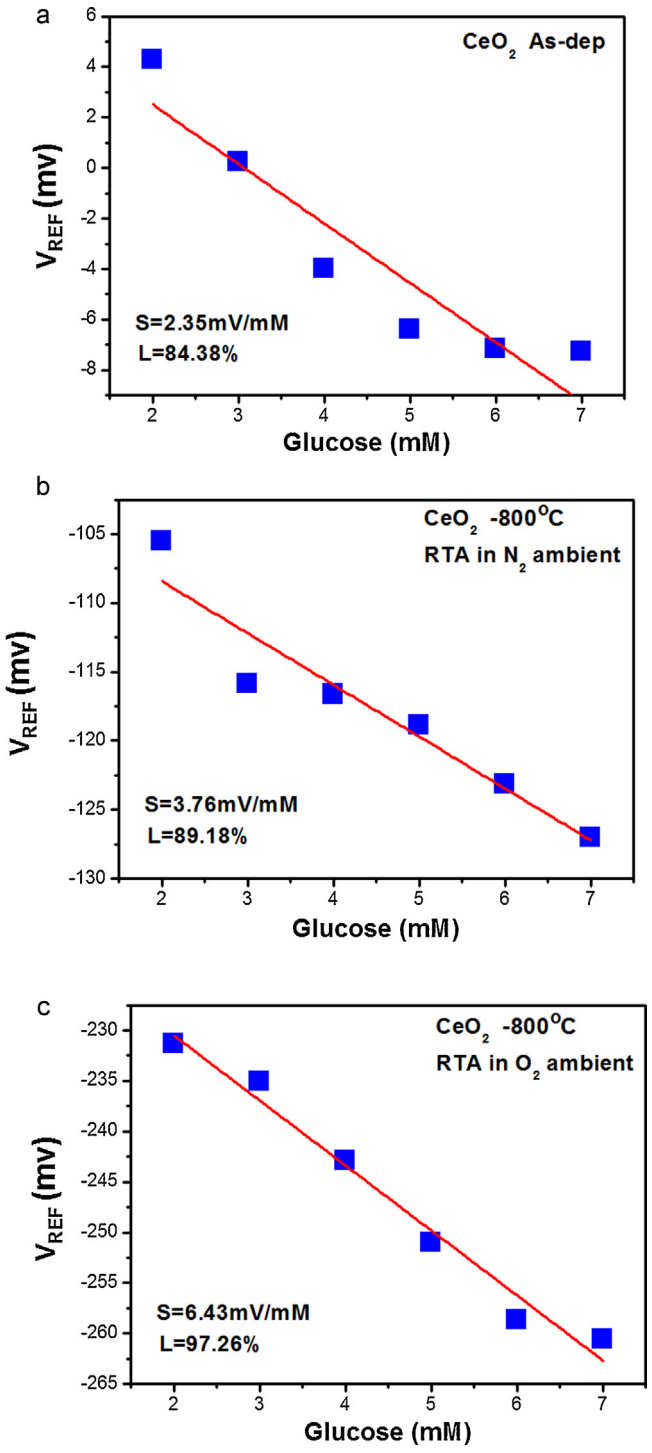

Fig. 10. Glucose responses from (a) the as-deposited CeO_2 sensing membrane (b) the membrane annealed at 800 °C in N_2 ambient (c) the membrane annealed at 800 °C in O_2 ambient.

sensing properties than all the other samples. In addition, to investigate the glucose sensing properties of the CeO_2 sensing membrane on EIS structure, a glucose solution with concentration in a range between 2 and 7 mM was prepared. In Fig. 10(a) and (b), it can be seen that the sensibility values of the as-deposited sample and annealed samples with RTA at 800 °C in O_2 and N_2 ambient were 1.49, 3.73, and 3.55 mV/mM, respectively. The linearity values of the as-deposited sample and annealed samples with RTA at 800 °C in O_2 and N_2 ambient were 63.19%, 97.26%, and 89.18%, respectively. In line with H^+, K^+, and Na^+ sensing results, the sample annealed at 800 °C in O_2 ambient had the highest sensitivity and linearity for urea and glucose sensing because of the improvements of the material property.

4. Conclusion

In this study, we fabricated an EIS sensor with a CeO_2 sensing membrane treated with annealing in O_2 and N_2 ambient on a

silicon substrate for pH sensing. The material properties of CeO_2 films were investigated by XRD, XPS and AFM analyses. In addition, all other sensing capability, including the hysteresis voltage and the drift rate, could be achieved at an optimal temperature of 800 °C, while the CeO_2 sensing membrane after annealing in O_2 ambient also showed better properties than the sample in N_2 ambient. The sensing performance of CeO_2-based EIS sensors for various concentrations of Na^+, K^+, urea, and glucose was tested. CeO_2-based EIS sensors show promises for the future applications of bio-medical device.

References

[1] P. Bergveld, Development of an ion-sensitive solid state device for neuro physiological measurement, IEEE Trans. Biomed. Eng. 17 (1970) 70–71.
[2] L.T. Yin, J.C. Chou, W.Y. Chung, T.P. Sun, S.K. Hsiung, Separatestructure extended gate H^+-ion sensitive field effect transistor on a glasssubstrate, Sens. Actuators, B 71 (2000) 106–111.
[3] H.K. Liao, J.C. Chou, W.Y. Chung, S.K. Hsiung, Proceeding of the Third East Asian Conference on Chemical, Sensor, Seoul, South Korea, 1997.
[4] L.L. Chi, J.C. Chou, W.Y. Chung, T.P. Sun, S.K. Hsiung, Study on extended gate field effect transistor with tin oxide sensing membrane, Mater. Chem. Phys. 63 (2000) 19–23.
[5] H.K. Liao, J.C. Chou, W.Y. Chung, Study of amorphous tin oxide thin films for ISFET applications, Sens. Actuators, B 50 (1998) 104–109.
[6] S. Jamasb, S. Collins, R.L. Smith, A physical model for drift in pH ISFETs, Sens. Actuators, B 15 (1997) 1379–1382.
[7] B.T. Radhouane, B. Takayuki, O. Yutaka, T. Yasutaka, Tin doped indium oxide thin films: electrical properties, J. Appl. Phys. 83 (1998) 2631–2645.
[8] C.H. Kao, C.C. Chen, C.H. Huang, C.Y. Huang, C.J. Lin, J.C. Ou, Investigation of Ti-doped Gd_2O_3 charge trapping layer with HfO_2 blocking oxide for memory application, Thin Solid Films 520 (2012) 3857–3861.
[9] C.H. Kao, H. Chen, C.S. Lai, J.C. Wang, S.P. Lin, K.S. Chen, C.Y. Huang, J.C. Ou, Erbium oxide as pH-sensing membranes in extended gate field effect transistors, Adv. Sci. Lett. 5 (2012) 1–4.
[10] N.S. Arul, D. Mangalaraj, T.W. Kim, Photocatalytic degradation mechanisms of self-assembled rose-flower-like CeO_2 hierarchical nanostructures, Appl. Phys. Lett. 102 (2013) 223115-1–223115-4.
[11] N. Izu, T. Itoh, W. Shin, I. Matsubara, N. Murayama, CO sensor having two Zr-doped CeO_2 films with and without catalyst layer, Electrochem. Solid-State Lett. 10 (2007) J37–J40.
[12] X.Q. Fu, C. Wang, H.C. Yu, Y.G. Wang, T.H. Wang, Fast humidity sensors based on CeO_2 nanowires, Nanotechnology 18 (2007) 145503-1–145503-4.
[13] A.A. Ansari, P.R. Solanki, B.D. Malhotra, Sol–gel derived nanostructured cerium oxide film for glucose sensor, Appl. Phys. Lett. 92 (2008) 263901–263903.
[14] M. Faisal, S.B. Khan, M.M. Rahman, A. Jamal, K. Akhtar, M.M. Abdullah, Role of ZnO–CeO_2 nanostructures as a photo-catalyst and chemi-sensor, J. Mater. Sci. Technol. 27 (2011) 594–600.
[15] Y. Nishikawa, T. Yamaguchi, M. Yoshiki, H. Satake, N. Fukushima, Interfacial properties of single-crystalline CeO_2 high-*k* gate dielectrics directly grown on Si (1 1 1), Appl. Phys. Lett. 81 (2002) 4386–4388.
[16] T.F. Lu, C.M. Yang, J.C. Wang, K.I. Ho, C.H. Chin, D.G. Pijanowska, B. Jaroszewicz, C.S. Lai, Characterization of K^+ and Na^+-sensitive membrane fabricated by CF_4 plasma treatment on hafnium oxide thin films on ISFET, J. Electrochem. Soc. 158 (2011) J91–J95.
[17] C.E. Lue, T.C. Yu, C.M. Yang, D.G. Pijanowska, C.S. Lai, Optimization of urea-EnFET based on Ta_2O_5 layer with post annealing, Sensors 11 (2011) 4562–4571.
[18] H.D. Jang, S.K. Kim, H. Chang, K.M. Roh, J.W. Choi, J. Huang, A glucose biosensor based on TiO_2–graphene composite, Biosens. Bioelectron. 38 (2012) 184–188.
[19] H.D. Kim, S.W. Jeong, M.T. You, Y. Roh, Effects of annealing gas (N_2, N_2O, O_2) on the characteristics of $ZrSi_xO_y/ZrO_2$ high-*k* gate oxide in MOS devices, Thin Solid Films 515 (2006) 522–525.
[20] M.J. Abdullah, A.A. Aziz, N.H. Al-Hardan, S.A. Rosli, Effect of N_2 and O_2 anneal gas ratio for low resistance p-type ZnO formation, in: ICSE2006, Kuala Lumpur, Malaysia, 2006.
[21] C.H. Kao, H. Chen, J.S. Chiu, K.S. Chen, Y.T. Pan, Physical and electrical characteristics of the high-*k* Ta_2O_5 (tantalum pentoxide) dielectric deposited on the polycrystalline silicon, Appl. Phys. Lett. 96 (2010) 112901-1–112901-3.
[22] Z. Wang, C. Zhao, P. Yang, L. Winnubst, C. Chen, Effect of annealing in O_2 or N_2 on the aging of $Fe_{0.5}Mn_{1.84}Ni_{0.66}O4$ NTC-ceramics, Solid State Ionics 177 (2006) 2191–2194.
[23] C.C. Wang, L.W. Zhang, Oxygen-vacancy-related dielectric anomaly in $CaCu_3Ti_4O_{12}$: post-sintering annealing studies, Phys. Rev. B: Condens. Matter 74 (2006) 024106-1–024106-4.
[24] F. Roch-Ramel, An enzymatic and fluorophotometric method for estimating urea concentrations in nanoliter specimens, Anal. Biochem. 21 (1967) 372–381.
[25] H. Scher, E.W. Montroll, Anomolous transit-time dispersion in amorphous solids, Phys. Rev. B: Condens. Matter 12 (1975) 2455–2477.
[26] G. Pfister, H. Scher, Time-dependent electrical transport in amorphous solids: As_2Se_3, Phys. Rev. B: Condens. Matter 15 (1977) 2062–2083.
[27] H. Barhoumi, A. Maaref, M. Rammah, C. Martelet, N. Jaffrezic, C. Mousty, S. Vial, C. Forano, Urea biosensor based on Zn_3Al–urease layered double hydroxides nanohybrid coated on insulated silicon structures, Mater. Sci. Eng., C 26 (2006) 328–333.
[28] N.H. Chou, J.C. Chou, T.P. Sun, S.K. Hsiung, Study on the disposable urea biosensors based on PVC–COOH membrane ammonium ion-selective electrodes, IEEE Sens. J. 6 (2006) 262–268.
[29] A. Maaref, H. Barhoumi, M. Rammah, C. Martelet, N. Jaffrezic-Renault, C. Mousty, S. Cosnier, Comparative study between organic and inorganic entrapment matrices for urease biosensor development, Sens. Actuators, B 123 (2007) 671–679.
[30] M. Singh, N. Verma, A.K. Garg, N. Redhu, Urea biosensors, Sens. Actuators, B 134 (2008) 345–351.
[31] G. Dhawan, G. Sumana, B.D. Malhotra, Recent developments in urea biosensors, Biochem. Eng. J. 44 (2009) 42–52.
[32] T.M. Pan, M.D. Huang, W.Y. Lin, M.H. Wu, A urea biosensor based on pH-sensitive $SmTiO_5$ electrolyte–insulator–semiconductor, Anal. Chim. Acta 669 (2010) 68–74.
[33] T.M. Pan, M.D. Huang, C.W. Lin, M.H. Wu, Development of high-*k* $HoTiO_3$ sensing membrane for pH detection and glucose biosensing, Sens. Actuators, B 144 (2010) 139–145.

Biographies

Chyuan Haur Kao was born in Taipei, Taiwan, 1966. He received the M.S. degree from the Department of Electric Engineering, National Cheng Kung University, Taiwan, in 1990 and the Ph.D. degree from the Institute of Electronics, National Chiao Tung University, Taiwan, in 1997. In 2005, he joined the faculty at Chang Gung University as an assistant professor in the Department of Electronics Engineering. He is a professor in that department and his current research areas focus on the high-*k* gate dielectrics, flash memories, and extended-gate field-effect transistors.

Hsiang Chen was born in Taipei, Taiwan, 1973. He received the B.S. and M.S. degree from the Department of Electric Engineering, National Taiwan University, Taiwan in 1995 and 1997. He received the Ph.D. degree from University of California, Irvine in 2008. In 2008, he joined the faculty at National Chi Nan University, Taiwan and became an associate professor in 2011. His current research areas focus on the high-*k* gate dielectrics, extended-gate field-effect transistors, and GaN optoelectronics.

Ming-Ling Lee received her B.S. and M.S. degrees in Department of Physics from National Cheng Kung University, Taiwan in 1991 and 1993, respectively. Since 2011, she has been working toward Ph.D. degrees in the Department of Electronic Engineering at National Chiao Tung University, Hsinchu, Taiwan. Her research interests include physics, technologies, Nano-devices and bio-sensor, EIS sensor.

Che-Chung-Liu was born in ILAN, Taiwan, on May 7, 1989. He received the bachelor's degree in electronic engineering from Ming Chuan University in June 2011. Since 2011, he has been working toward master's degree in the Department of Electronic Engineering at Chang Gung University. His research interests include the fabrication and measurement of high-*k* materials applied in bio-sensors, EIS sensor, EGFET sensors.

Herng-Yih Ueng engages in the photovoltaic cell and applications more than 30 years from 1982 to 2013. Since the first paper of amorphous thin film for solarcell (1984 IEEE specialist Conference) to High efficiency amorphous solar cell in theoretical approach (Physics of semiconductor 22th conference, Greece), some of the photovoltaic materials such Si, CdTe, CIS, and GaSb/GaAs or InAs/GaAs Quantum dots were carried out being processed by MBE and electrodepositing process. Recently, a more convenient deposition process, electrodeposition technology have been developed for DLC materials, focus on the nanoscale applications such as the biomedicalcoating implant and the biomaterials. In particular, as the photovoltaic cell.

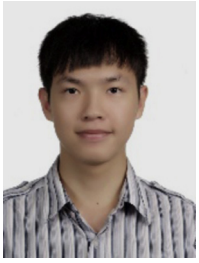

Yu-Cheng Chu was born in Taipei, Taiwan, in 1990. He received the bachelor's degree in electronic engineering from National Quemoy University in June 2012. Since 2012, he has been working toward master's degree in the Department of Applied Materials and Optoelectronic Engineering at National Chi Nan University. His research interests include LED reliability, sensor and flash memory.

Ching-Bang Chen was born in Taichung, Taiwan, in 1989. He received a B.S. in Applied Materials and Optoelectronic Engineering from National Chi Nan University in June 2013. His research interests include the characterization of biosensor and LED.

Kow-Ming Chang received the B.S. degree (with great distinction) in chemical engineering from National Central University, Chung-Li, Taiwan, in 1977 and the M.S. and Ph.D. degrees in chemical engineering from the University of Florida, Gainesville, in 1981 and 1985. His current research interests include physics, technologies, and modelling of heterojunction devices and optoelectronic devices, ULSI key technologies, Nano-CMOS, TFT, and MEMS devices and technologies.